Quadrupole Coupling Constants C_{QQ} for ^{2}H, ^{27}Al, and ^{17}O Atoms Calculated at the Periodic Hartree–Fock Level for Understanding the Geometry of H-Form Aluminosilicates

A. V. LARIN,[1] D. P. VERCAUTEREN[2]

[1]*Laboratory of Molecular Beams, Department of Chemistry, Moscow State University, Vorob'evu Gory, Moscow, B-234, 119899, Russia*

[2]*Institute for Studies in Interface Sciences, Laboratoire de Physico-Chimie Informatique, Facultés Universitaires Notre Dame de la Paix, Rue de Bruxelles 61, B-5000 Namur, Belgium*

Received 6 November 2000; revised 26 January 2001; accepted 5 February 2001

ABSTRACT: The coordinates of crystallographically different atomic types of Si–O(H)–Al Brönsted centers within five H-form aluminosilicate frameworks—ABW, CAN, CHA, EDI, and NAT—were optimized using a full periodic ab initio Hartree–Fock scheme at the STO-3G level. Single-point calculations were then carried out at the ps-21G*(Al, Si)/6-21G*(O, H) and 6-21G*(Al, Si)/6-21G*(O, H) levels to obtain the ^{2}H, ^{27}Al, and ^{17}O respective nuclear quadrupole coupling constants and electrostatic field gradient anisotropies. The latter are discussed and compared to the experimental values measured for different zeolites. Int J Quantum Chem 82: 182–192, 2001

Key words: quadrupole coupling constants; H-forms; aluminosilicates; Hartree–Fock theory

Correspondence to: D. P. Vercauteren; e-mail: vercau@scf.fundp.ac.be.

Contract grant sponsor: Interuniversity Research Program.
Contract grant number: PAI/IUAP 4/10.

Introduction

Detailed analyses of the spatial characteristics of the most efficient known zeolite precursors surely can help the synthesis of perspective new catalyst materials. More particularly in the special case of H-form aluminosilicates, applied in important industrial methanol to gasoline (MTG) and catalytic cracking processes [1], the structure of the active bridged Si–O(H)–Al moiety can be studied by combining nuclear magnetic resonance (NMR) and theoretical methods [2]. The direct relation between the quadrupole coupling constant (C_{QQ}) of the atoms constituting the framework and the electrostatic field gradient, indeed, makes the C_{QQ} constant a valuable source of data on the field gradient, which is directly related to the respective atomic environment. The interest for such theoretical studies is, moreover, increased owing to the problematic determination of the electrostatic field gradient (EFG) values from X-ray data [3] as compared, for example, to the electrostatic potential (EP) evaluation [4]. The experimental EFG data at the framework atoms are preferable for the assertion of the derivatives of the EP as compared to any other source of experimental data, i.e., the infrared (IR) estimation of the electrostatic field at the positions of small adsorbed probes. The field should be assigned to the positions of the probes that require the determination of the adsorbate–adsorbent potential and adsorbate location [5, 6], while the positions of the framework nuclei are usually well known. As a result, considering periodic Hartree–Fock (PHF) methods for the calculation of the electrostatic field presents some advantages as compared to IR estimations.

Various ways to evaluate the EP have been proposed since the 1970s. One of them, proposed by Stewart [4], is based on the calculation of multipole moments (MM) of high orders on the basis of X-ray data. Within this method, the fitting parameters are the atomic MM values. Recently, Larin et al. [7] showed that correlations between the MMs, including the neighbor atoms, and without addressing the experimental electron density from X-ray data, is also very useful for the calculation of the MM of high orders. The particular interest for such MM relations is that they are particularly suitable to tackle frameworks that cannot be treated with PHF schemes owing to a large number of atoms per unit cell (UC). These relations could also be considered for systems possessing some unordered cations or hydrogen atoms. In these frameworks, fitting the positions and MMs for the constituting atoms from X-ray experiment is indeed a problem often encountered.

The method to calculate MMs for "large" zeolites is indirectly based on the proposition that the TO_4 units in "small" or "large" frameworks are embedded in essentially the same media and their characteristics could, hence, be discussed within a common approach of MM analysis, i.e., MM dependences on both the geometry and low-order MMs can be described by common functions [7]. However, a comparison between all measured characteristics of the possible different frameworks is desirable to confirm the identity or closeness of the electrostatic field values. Also, the basis sets applied to obtain the MM dependences should be tested to provide a sufficiently precise correlation with available relevant experimental data.

In this study, we first will shortly present the adopted computational strategy. The main geometrical features of the optimized models are discussed below. The discussion is devoted to the results of the calculations of the nuclear quadrupole coupling constants (C_{QQ}) and the EFG anisotropy of the quadrupolar nuclei, ^{2}H, ^{27}Al, and ^{17}O, respectively, for five H-form zeolites (ABW, CAN, CHA, EDI, and NAT) as well as to the comparison with experimental data available for zeolites possessing "large" unit cells (ZSM-5 and Y zeolite).

Computational Strategy

The theoretical bases for the solution of the Schrödinger electronic problem in three dimensions considering periodic boundary conditions have already largely been described in the literature [8, 9]. In this work, we optimized the fractional coordinates of the different Brönsted centers, i.e., the Si–O(H)–Al moieties, for a series of five cationic forms of aluminosilicate, with a relatively small number of atoms per unit cell, i.e., ABW [10], CAN [11], CHA [12], EDI [13], and NAT [14] (Table I), using a full periodic Hartree–Fock CO-LCAO-SCF scheme. Respective low symmetry groups were held for the optimization because they allow to consider nonequivalent Al and Si positions. Starting from initial cationic forms, one could avoid appreciable variations of the cell volume when replacing a cation by a bridged hydrogen atom. The cell parameters could, hence, be kept fixed. For all five frameworks, we allowed the variation of the coordinates of the four (O, H, Si, Al) framework atoms involved in each

TABLE I

Symbol, number of atoms, of different Al, Si, and O types ($n_H = n_{Al}$), of atomic orbitals (AO) per unit cell (UC), and symmetry group of the H-form aluminosilicates.[a]

Name	Symbol	Atoms (UC)	$n_{Al}/n_{Si}/n_O$	AO/UC (6-21G**)	Symmetry group
ABW	HABW	28	1/1/4	388	$Pna2_1$
Cancrinite	HCAN	42	1/1/4	582	$P6_3$
Chabazite	HCHA	39	1/3/8	517[a]	R3
Edingtonite	HEDI	34	1/2/5	480	$P2_12_12$
Natrolite	HNAT	34	1/2/5	480	Fdd2

[a] With the ps-21G** basis set.

type of bridged Brönsted center (12 variables) [15]. In the case of HEDI, the optimization of the same fractional coordinates allowing the additional variation of the cell parameters was also considered for comparison. [Note: In this article, we will show that their influence on the final geometry is of lower significance.] The optimizations were carried out, with CRYSTAL95 [16] in which we implemented the Polak–Ribiere algorithm [17], with energy convergences of 10^{-3} kcal/mol. The minimal STO-3G basis set was chosen to handle a reasonable number of atomic orbitals (AO) per UC, hence leading to moderate computing times. Using the optimized geometry, single-point calculations were then considered with the ps-21G*(Al, Si)/6-21G*(O, H) and 6-21G*(Al, Si)/6-21G*(O, H) basis sets (named hereafter as ps-21G** and 6-21G**, respectively) to obtain the atomic nuclear quadrupole coupling constants (C_{QQ}) of ^{2}H, ^{27}Al, and ^{17}O, as well as the EFG tensor elements at their respective locations, as implemented in the CRYSTAL code.

With the ps-21G** basis, the SCF part converged properly for each of the four different TO_4 moieties in all the five H-forms, i.e., 20 cases in total. The exponents used for the 3*sp*′ orbitals of Si and Al were 0.12339 and 0.17 a.u.$^{-2}$, respectively, and that for the 2*sp*′ orbital of O was 0.3737 a.u.$^{-2}$. The exponents for the *d* polarization functions of Al, Si, and O were optimized as 0.45, 0.5, and 0.6 a.u.$^{-2}$, respectively. The *sp*/*d* exponents used for the 6-21G** basis are 0.9, 0.15/0.35, 0.15/0.4, and 0.42/0.72 a.u.$^{-2}$ for the H, Al, Si, and O atoms, respectively. With the 6-21G** basis, the SCF convergence was achieved in 9 among all 20 optimized Si–O(H)–Al moieties.

All computations with the CRYSTAL95 code were carried out on an IBM 15-node (120 MHz) Scalable POWERparallel platform (with 1 Gb of memory/CPU). In all cases, the thresholds for the calculations were fixed to 10^{-5} for the overlap coulomb, the penetration coulomb, and overlap exchange, to 10^{-6} and 10^{-11} for the pseudo-overlap exchange, and to 10^{-5} for the pseudopotential series for all levels of basis sets. A typical total geometry optimization of one bridged Brönsted center (12 variables) with the STO-3G basis set took 2–3 days on the above-cited CPU. Single-point computations with the split-valence bases were executed directly without keeping the bielectronic integrals. The respective shortest SCF convergence (7–8 cycles) took around 1.5–2 h in the case of the Brönsted centers of the HABW zeolite.

The nuclear C_{QQ} characterizes the quadrupole interactions of an asymmetric nucleus. The C_{QQ} values (in MHz) for all atoms within the five H-forms were obtained using the EFG values at their respective positions [16]:

$$C_{QQ} = 2.3496 \times 10^2 Q \nabla E_{zz}, \quad (1)$$

where the coefficient on the right hand-side corresponds to ∇E_{zz} expressed in $e \times$ a.u.$^{-3}$, and the nuclear quadrupole moments Q are 0.1402 [18], −0.026 [19], and 0.00286 [20, 21] barn (1 barn = 10^{-28} m^2) for ^{27}Al, ^{17}O, and ^{2}H, respectively. Another parameter that influences the spectra of a nucleus having a quadrupolar nuclear moment is the EFG anisotropy:

$$\eta = (\nabla E_{xx} - \nabla E_{yy})/\nabla E_{zz}, \quad (2)$$

wherein all EFG elements are related to the EFG tensor principal axes.

Results

GEOMETRY OPTIMIZATIONS

The variations of the structural characteristics of the bridged moieties while optimizing the fractional coordinates of each crystallographically different atomic type of Brönsted center were already discussed earlier [15]. The variety of the models considered covers a wide range of Al–O and Si–O distances, Si–O–Al angles, and H deflection angles from the Si–O–Al plane. Here, for conciseness, we only discuss the more recent geometries obtained considering the additional variation of the cell parameters for the HEDI case by comparison with the previous optimization based on the fractional coordinates of the bridged atoms only (Table II). The first observation is that even if the relative energies obtained, varying both the fractional coordinates and cell parameters, qualitatively repeat the *ratio* obtained earlier, varying the fractional coordinates only [15], the spatial characteristics of the Si–O(H)–Al moieties between the O(1) and O(4) types become closer. Second, the simultaneous increase of both the Si–O–Al angle and the H de-

TABLE II

Geometry of the Brönsted sites (distances in Å, angles in degrees), for HEDI optimized with the STO-3G basis set varying either the fractional coordinates (FC) of the H, O, Si, and Al atoms only (upper part) or the FC together with the cell parameters (lower part, with cell parameters *a*, *b*, *c*, in Å, and change of volume ΔV of unit cell, in %).[a]

	Fractional coordinates (FC)			
Parameters	O(3)	O(4)	O(2)	O(1)
Si–O–Al initial	134.76	138.27	132.47	143.38
Si–O–Al opt.	135.41	129.10	142.00	139.26
O–H	0.970	0.983	0.971	0.983
Si–O	1.775	1.827	1.746	1.676
Al–O	1.845	1.906	1.829	1.913
Al–H	2.396	2.493	2.353	2.463
β[b]	3.7	0.3	1.2	0.4
Si–O–H	111.6	115.3	107.5	108.2
Al–O–H	112.9	115.6	110.5	112.5
$\Delta U_{STO\text{-}3G}/\Delta U_{ps\text{-}21G^*}$	0.0/0.0	15.4/14.1	16.1/34.2	62.4/59.3
	FC + cell parameters			
Parameters	O(3)	O(4)	O(2)	O(1)
Si–O–Al initial	135.41	129.10	142.00	139.26
Si–O–Al opt.	137.76	137.51	142.84	141.27
O–H	0.976	0.975	0.974	0.978
Si–O	1.740	1.748	1.715	1.680
Al–O	1.830	1.827	1.796	1.865
Al–H	2.377	2.343	2.287	2.377
β[b]	6.8	6.0	14.9	6.4
Si–O–H	109.7	112.6	108.3	109.0
Al–O–H	112.2	109.7	107.6	109.5
a[c]	9.490	9.448	9.320	9.429
b	9.455	9.555	9.585	9.662
c	6.363	6.430	6.503	6.376
$-\Delta V$	7.92	3.59	3.51	3.52
$\Delta U_{STO\text{-}3G}$	0.0	9.4	27.5	68.9

[a] Relative energies (in kcal/mol) are also given for the ps-21G*(Al, Si)/6-21G*(O, H) basis set.
[b] Angle (in degrees) of the H deflection form the Si–O–Al plane.
[c] Initial values of *a*, *b*, and *c* are 9.55, 9.665, and 6.523 Å, respectively [13].

flection angle from the Si–O–Al plane for all centers together with the cell parameters decrease was not predictable. One could indeed expect a smaller Si–O–Al angle while decreasing the cell parameters. The Al–H distance, considered as one of the most reliable geometric parameters of the Si–O(H)–Al moiety from the experimental point of view, also shortens as compared to the lower experimental estimate 2.37 ± 0.04 [22] observed for the bridged groups in the 6-membered rings of zeolite HY or to even a smaller value for O(2) in HEDI.

The decrease of the cell volume does not exceed 8% while adding H to the Si–O(3)–Al moiety as compared to the initial cationic EDI form, and it is smaller than 4% for the other Si–O(H)–Al groups (Table II). This is appreciably smaller and opposite to the increase by 14% noted by Ugliengo et al. [23] while optimizing the replacement of Si by (Al + H) starting from an initial all-siliceous EDI structure using the GULP code [24] based on B3LYP parameterization.

Total optimizations, i.e., coordinates of all atoms and cell parameters, for the other HABW, HNAT, and HCAN frameworks were not completed, but we can confirm that the decrease of their cell volume starting from their cationic form is even smaller than for the HEDI case. Cationic models are thus more appropriate initial structures as compared to their all-siliceous analogs for the optimization of the H-forms because they require a smaller variation of the cell parameters. This tendency should, however, be evidently tested with a higher quality basis set level.

QUADRUPOLE COUPLING CONSTANTS OF THE DEUTERIUM ATOMS

For ^{2}H, while the EFG anisotropies at the positions of the different crystallographically independent types of H are in agreement with the measured value 0.1 ± 0.05 [25], the calculated $C_{QQ}(^2H)$ values (circles in Fig. 1) are usually overestimated by 25–30% as compared to the experimental ones for HY and HZSM-5 forms [2, 25, 26] (dashed lines in Fig. 1). The reason for the relatively large difference between experiment and calculation can come either from overestimated nuclear quadrupole moments Q, or from a wrong geometry accepted for the interpretation. Allowing the high computation accuracy of the nuclear quadrupole ^{2}H moment Q, i.e., ±0.7% [20], one hence can only discuss the problem from the point of view of geometry.

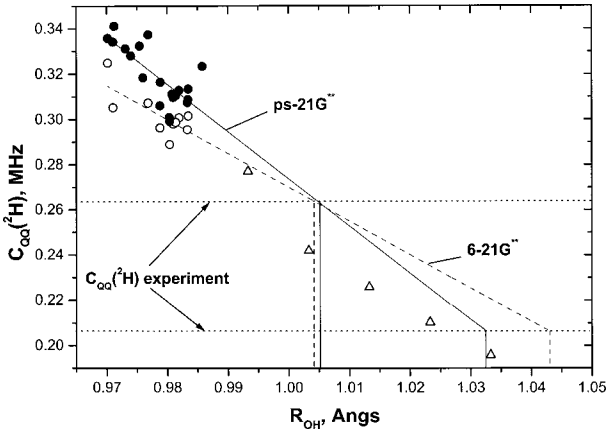

FIGURE 1. $C_{QQ}(^2H)$ (in MHz) calculated with the ps-21G** (filled circles) and 6-21G** (open circles for all models and triangles for the Si–O_1(H)–Al moiety with elongated O_1–H bond within HEDI) basis sets for the five H-form aluminosilicates with respect to O–^{2}H bond length (Å). Interval of experimental data [2, 25, 26] is limited by dashed lines.

The $C_{QQ}(^2H)$ values, which decrease with the O–^{2}H bond length with both ps-21G** and 6-21G** basis sets, are relatively close for all different ^{2}H atoms, which thus indicates that the replacement of the core electrons of the remoted Si and Al by pseudopotentials has no influence. We also extrapolated the $C_{QQ}(^2H)$ values for longer O–^{2}H bond lengths (lines in Fig. 1) as compared to that optimized, with cluster or periodic calculations, in the O–H case. To verify such extrapolation, we calculated the $C_{QQ}(^2H)$ values with 6-21G** for the Si–O_1(H)–Al moiety of HEDI. This moiety was chosen as it corresponded closely to the cluster geometry case: |O–H| = 0.983, |O–Si| = 1.676, |O–Al| = 1.913 Å, and β = 0.4°. The interval for the O–H bond length variation was chosen between 0.9933 and 1.0333 Å (triangles in Fig. 1), while all other structural parameters (the |O–Si| and |O–Al| distances, as well as the H–O–Si, H–O–Al, and Al–O–Si angles) were kept fixed. A satisfactory agreement with the measured $C_{QQ}(^2H)$ values, between 208 and 264 kHz [2, 25, 26], was obtained for the shortest O–^{2}H bond lengths, between 0.9933 and 1.025 Å, as compared to what could be predicted from the extrapolated values, between 1.005 and 1.043 Å (6-21G** level).

The $C_{QQ}(^2H)$ and $\eta(^2H)$ variations with the H deflection angle β from the Si–O_1(H)–Al plane were also tested, but they are negligible. So, a longer O–^{2}H bond length can explain the difference between the theoretical and experimental $C_{QQ}(^2H)$

values. This difference could be explained taking into account that the experimental $C_{QQ}(^2H)$ and O–^{2}H bond values are measured at the averaged ground state value R_0 as compared to the equilibrium value R_e usually obtained via ab initio computations. This larger value is confirmed by the experimental value of 1.051 Å for the O–H bond in zeolite Y obtained from inelastic neutron scattering experiment [27]. Hence, we decided to check the possible anharmonic increase of the O–H bond length of a bridged moiety in the v-vibrational state as [28]:

$$R_v = R_e - (3aB_eR_e/\omega_e)\left(v + \tfrac{1}{2}\right), \qquad (3)$$

where the anharmonicity coefficient a is $-2.210/-2.466$, the rotational constant B_e is 18.825/10.028, and the harmonic frequency ω_e is 3727/2721.2 cm^{-1} for the O–H/O–^{2}H bond lengths, respectively, [29]. Using these values, one could evaluate the increase at the ground vibrational state, $\Delta R_0 = R_0 - R_e$, as around 0.0162/0.0273 Å. The larger anharmonicity correction for the O–^{2}H bond is in agreement with the known longer O–^{2}H bond lengths [30]. So, if an equilibrium O–^{2}H value R_e of 0.97–0.98 Å is obtained via any optimization scheme, then the resulting ground-state distance provides, owing to the O–^{2}H anharmonicity, a decrease of $C_{QQ}(^2H)$ to 208–264 kHz, which is in the usual range of the experimental estimates for the H-forms [2, 25, 26]. The reason for a smaller length R_0 obtained via Eq. (3) as compared to the average experimental value 1.051 Å [27] could be discussed knowing the respective experimental error values, but no values were presented in Ref. [27].

Another important question is the influence between the local characteristics such as the O–H frequency [31 – 34] or the O–H bond length [23, 33] and the geometry of the bridged moiety. So far, to our knowledge, the influence of the local geometry was usually limited to the Si–O–Al angle (ϑ) omitting the other local characteristics. Particularly, several authors showed that the O–H frequency [32, 34] badly correlates with the ϑ angle in a series of H-forms of SAPO (based on the ALPO-5 and ALPO-34 sieves [32]) as well as in aluminosilicates (SSZ-13, SSZ-24 [32], MCM-22 [34]) empirically optimized with GULP [24] considering both empirical and ab initio based force fields. These results were supposed to be sufficient to conclude to a domination of the long-range effects on the O–H frequency. An opposite conclusion about the existence of the ϑ dependence on the O–H frequency, although not very precise, was observed in HSAPO-34 using a plane wave approach [31]. A last example of the importance of the local characteristics was demonstrated via a quadratic dependence of the O–H bond length on the ϑ angle for HEDI optimized with GULP applying a parameterization based on B3LYP calculations [23].

The influence of the electron correlation on the EFG values can be estimated as rather small by comparison with the corresponding values recently published for the HEDI structure [35]. From our calculated $C_{QQ}(^2H)$ values (Fig. 1), one estimated, using expression (1), that the respective EFG value ranges are 43.4–49.2 Å^{-2} and 41.9–47.7 Å^{-2} for the H-forms studied herein with Si/Al ratio between 1 and 2 at the ps-21G** and 6-21G** basis set levels, respectively. This is in good agreement with the approximate interval 42.5–43.5 Å^{-2} calculated with B3LYP for HEDI structures with Si/Al ratio between 1 and 3 [23].

One could thus suggest that a more precise coordinate dependence should be proposed to reveal the real influence of the local moiety on the O–H characteristics. For a complete conclusion, the influence of all other local characteristics, like the β angle of the proton deflection from the Si–O–Al plane, should also be checked. As soon as the electrostatic field at the proton position correlates with the O–H frequency [32, 33], the field value should, indeed, also depend on the local coordinates. We thus verified this dependence avoiding the problem of the O–H frequency calculation with the usual wave functions as applied in CRYSTAL. The field vector was calculated at the H position while the latter was allowed to "move" along the angle β with respect to the Si–O(1)–Al plane within the HEDI framework. The most favored H position in this grid is 6.0° with the 6-21G** basis set, which coincides to 6.24° fitted with STO-3G while varying the cell parameters (lower part of Table II). The barrier of the β vibration (Fig. 2) is lower than 70 K $= 2.2 \times 10^{-4}$ a.u. for a motion between 6° and −2° and lower than 163 K $= 5.2 \times 10^{-4}$ a.u. between 6° and 20°, so that the β motion relative to the plane is not strongly hindered within a wide temperature interval. The absolute value of the electrostatic field $|F| = 0.00575$ a.u. (or 29.57 V/Å) at $\beta = 6°$ varies up to 30% ($\beta = -2°$) and 31.5% ($\beta = 20°$). For comparison, the difference between the field values for the H atoms of all the bridged groups does not overhead ±8% relative to the average value [32, 34]. One should remark that the electrostatic field evaluation at the "cross" positions within the H-form of the MCM-22 zeolite, with ab initio based force fields [34], is close to our field

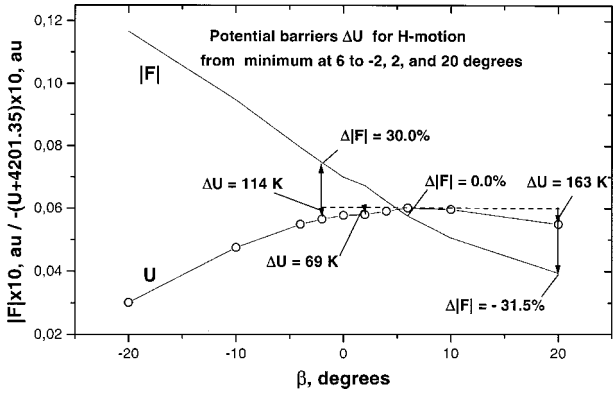

FIGURE 2. Absolute value of the electrostatic field $|F|$ ($\times 10$, a.u., solid line) at the proton position and total energy $U - 4201.35$ ($\times 10$, a.u., circles) with respect to the angle β (degrees) of the proton deflection from the Si–O(1)–Al plane within HEDI.

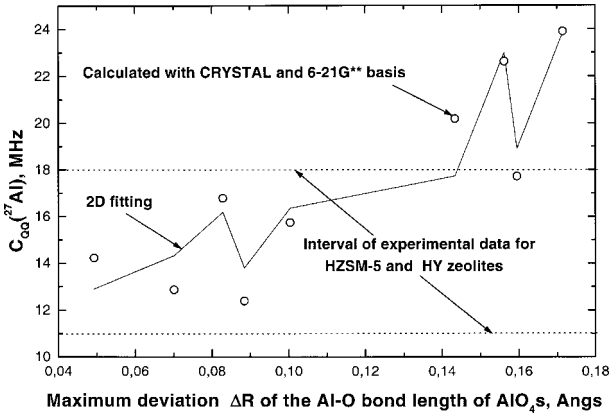

FIGURE 3. Approximation "$a_1 \sin(\varphi - \varphi_0) + a_2\,\Delta R^n + a_3$" (solid line) of the $C_{QQ}(^{27}\text{Al})$ (in MHz) calculated with 6-21G** (circles) for the four H-form aluminosilicates (excluding HCHA) with respect to the maximum deviation ΔR (in Å) of the O–Al bond length from the average AlO_4 value (Å) and to the maximal difference φ (in degrees) of the rows of the F_2-type deformational vibration of the AlO_4s. Interval of experimental data for HZSM-5 and HY zeolites [2, 25, 26] is limited by dashed lines.

estimation within HEDI, both being twice as large as the value obtained with empirical force fields.

Evidently, the optimization of the O–H bond length at different β angle values seems to decrease the field value as well as the barrier of the β vibration. But even after optimization (not performed here), the range of the field variation with β would remain appreciable with respect to the differences between its value at the different adsorption centers.

QUADRUPOLE COUPLING CONSTANTS OF THE ALUMINUM ATOMS

The same question of the choice of correct local coordinates discussed above for deuterium holds for aluminum. Both the deformational and stretching distortions lead to a symmetry lowering of the AlO_4 tetrahedra, which could lead to a variation of the C_{QQ} values. To our knowledge, only the deformational distortions were used so far to construct a local *shear strain* coordinate connecting any arbitrary AlO_4 distortion with the respective $C_{QQ}(^{27}\text{Al})$ value [36]. This coordinate is, however, only appropriate for cationic forms as studied in Ref. [36], wherein no particularly long O–Al bond appeared owing to the bridged O neighbor.

We performed a two-dimensional fitting with respect to the difference between the absolute values of the rows of both the deformational and stretching vibrational coordinates of the F_2 type. The valence and deformational types correspond to the rows of the irreducible representation of the F_2 type within the T_d point-symmetry group, that is, the stretching (valence) distortions $\Delta R = \max_{i,j}(a_i - a_j)$, $i, j = 1$–3, where $a_1 = \Delta r_1 + \Delta r_2 - \Delta r_3 - \Delta r_4$, $a_2 = -\Delta r_1 + \Delta r_2 + \Delta r_3 - \Delta r_4$, and $a_3 = \Delta r_1 - \Delta r_2 + \Delta r_3 - \Delta r_4$, in which $\Delta r_k = (r_k - R)$ is the displacement length of the k atom from the average value $R = (\sum r_m)/4$, and the angular (deformational) distortions $\varphi = \max_{i,j}(b_i - b_j)$, $i, j = 1$–3, where $b_1 = \Delta\alpha_{12} - \Delta\alpha_{34}$, $b_2 = \Delta\alpha_{23} - \Delta\alpha_{14}$, and $b_3 = \Delta\alpha_{13} - \Delta\alpha_{24}$, in which α_{kl} is the O_k–T–O_l angle between the bonds with k- and l-oxygen neighbors of each T atom ($k, l = 1$–4) and $\Delta\alpha_{kl} = \alpha_{kl} - 109°47$. The fitting with respect to the ΔR and φ parameters was, however, not successful; ΔR was then replaced by the largest deviation from the average AlO_4 value of the longest O–Al bond, so that $\Delta R = \max_i(r_i - R)$. Doing so, with a simple analytical form as "$a_1 \sin(\varphi - \varphi_0) + a_2\,\Delta R^n + a_3$," where a_i, n, and φ_0 are fitted parameters (note; this nearly arbitrary form was chosen to become zero for φ and ΔR approaching zero), led to a more reasonable agreement (Fig. 3). Most of the calculated points (circles in Fig. 3) are, indeed, within the range of the experimental evaluations from 11 to 18 MHz [2, 25, 26].

Let us add that applying the ps-21G** basis set on Al atoms was unsuccessful as it led to strongly underestimated $C_{QQ}(^{27}\text{Al})$ values. We did not find a simple *ratio* between the EFG anisotropy and the AlO_4 distortion and, hence, the results regarding η are not discussed herein.

TABLE III

EFG anisotropies η and $C_{QQ}(^{27}Al)$ values of the Al atoms whose calculated values do not coincide with the interval of experimental quadrupole coupling values with respect to the angular distortion $\varphi = \max_{ij}(b_i - b_j)$, $i,j = 1$–3, where b_i (in degrees) is a row of the irreducible representation for the deformational vibration of the F_2 type within the T_d point-symmetry group, and to the bond distortion $\Delta R = \max_i(r_i - R)$, $i = 1, 4$, R being averaged over $r_i = |Al–O_i|$ (all in Å) for the AlO_4 tetrahedra.

H-form	Nearest O(H) type	|Al–O(H)| (Å)	ΔR (Å)	R (Å)	φ (deg)	η	$C_{QQ}(^{27}Al)$ (MHz)
HNAT	O_4	1.836	0.143	1.692	7.53	0.601	20.2
HNAT	O_1	1.884	0.157	1.727	21.41	0.248	22.6
HEDI	O_1	1.913	0.171	1.741	16.85	0.184	23.9

So far, to our knowledge, $C_{QQ}(^{27}Al)$ values were measured for two Y and ZSM-5 zeolites only. Considering other zeolites could evidently shift the bounds of the experimental estimates of $C_{QQ}(^{27}Al)$. A relation between the AlO_4 distortion (as described by the structural φ and ΔR parameters) and the C_{QQ} values can, however, be preliminary discussed. Three C_{QQ} values are higher than 18 MHz and do not correspond to the measured values between 11 and 18 MHz [2, 25, 26]. Two of the three ^{27}Al atoms with the highest C_{QQ} values (22.6 and 23.9 MHz) in HEDI and HNAT frameworks are connected to the bridged moieties, which possess structural parameters that are close to the "cluster" model with an |O–Al| bond length of 1.90 Å (Table III). The smaller value of 20.2 MHz outside of the experimental limits corresponds to the typical Si–O(H)–Al moiety obtained with CRYSTAL at the STO-3G basis set level [12, 15] for an |O–Al| bond between 1.80 and 1.90 Å. So we can suggest that this long |O–Al| bond is responsible for the $C_{QQ}(^{27}Al)$ deviation out of the experimental range. Simultaneous verifications of the $C_{QQ}(^{27}Al)$ values with higher quality basis sets and further measurements of the $C_{QQ}(^{27}Al)$ range for other H-forms are thus necessary in order to discriminate between the different Al environments. One should mention that if we use the higher value $Q = 0.1466$ barn [37] recently obtained, $C_{QQ}(^{27}Al)$ values increase by 4.6% as compared to the value calculated with $Q = 0.1402$ barn [18]. It yields to 21.1, 23.6, and 25.0 instead 20.2, 22.6, and 23.9 MHz, respectively, in Table III.

Considering all possible H locations in the five frameworks, we obtained a wide variety of models of the bridged groups [15] as compared to the results of Teunissen, which optimized the HCHA framework at the same STO-3G level [12]. Together with the models with shorter Al–O distances usually obtained at this basis set level, a close cluster geometry was also obtained for several H positions in the HEDI, HCHA, and HNAT zeolites [15]. This shows the importance of the long-range contributions for the resulting geometries. In accordance with the C_{QQ} estimation [38] for the cluster geometry (respective model with |H–O| = 0.971, |Si–O| = 1.680, |Al–O| = 1.943 Å) at the 3-21G** level, we should have a correct C_{QQ} value (as compared to experiment) of about 14 MHz or less using $Q(^{27}Al) = 0.1402$ barn [18], because our H-form presents a lower |Al–O| distance (last line in Table III, |H–O| = 0.983, |Si–O| = 1.676, |Al–O| = 1.913 Å). But we obtained an overestimated $C_{QQ}(^{27}Al)$ value of 23.2 MHz with the 6-21G** basis.

The overestimation of the $C_{QQ}(^{27}Al)$ values calculated for the H-forms obtained via the isolated cluster approach as compared to the experimental ones was already discussed in the literature [38] allowing electronic correlation methods [second-order Møller–Plesset (MP2) or density functional theory (DFT)] and higher quality of basis sets. That is why we propose that more correct $C_{QQ}(^{27}Al)$ estimations owing to the long-range EFG contributions calculated within the PHF scheme could provide higher precision. We believe that the critics of the potential derived charge (PDC) model in [38] is not justified. The replacement of all electronic contributions to the EP by corresponding PDCs could be induced only for the remote electronic parts for which a presentation by a multipole series is appropriate as developed for example in [9]. Unfortunately, the limits of our available computational facilities did not allow us to test such possibilities of the PHF scheme with a higher quality basis.

QUADRUPOLE COUPLING CONSTANTS OF THE OXYGEN ATOMS

Results of the calculations of the C_{QQ} and ∇E_{zz} values with respect to the T–O–T′ angle are reciprocally inverted [Eq. (1)], so that analogous trends can be demonstrated either in terms of zeolite type (Fig. 4) or in terms of the T–O–T′ moiety (Fig. 5). Simple linear approximations "$\nabla E_{zz} = a \times \vartheta(^\circ) + b$," where $a = 7.5 \times 10^{-4}$, 1.47×10^{-3}, and -4.18×10^{-3} $e \times$ a.u.$^{-3} \times$ degree^{-1} and $b = 0.877$, 0.4873, and -0.7703 $e \times$ a.u.$^{-3}$ for the Si–O–Si, Si–O–Al, and Si–O(H)–Al types of oxygen, respectively, as given in Figure 5 (by dashed, dotted, and solid lines, respectively) can be converted to obtain the C_{QQ} values in Figure 4. However, the error of the respective fitting of the slope makes the ∇E_{zz} approximation to be only qualitative. The C_{QQ} values calculated herein for the Si–O–Si, Si–O–Al, and Si–O(H)–Al types of oxygen are partitioned from -5 to -6, -3.5 to -5, and 7.5 to 9 MHz, respectively. Absolute values of the Si–O–Si moiety are close to the experimental data obtained for all-siliceous faujasite [39], 5.1 to 5.39 MHz, or ferrierite [40], 5.22 to 5.64 MHz, while the experimental data for SiO_2 is near 5.8 MHz [41]. Other C_{QQ} data between 2.7 and 5.1 MHz were fitted from double rotation NMR spectra for a series of silicates [42]. The C_{QQ} values for the Si–O–Al moiety are relatively larger as compared to the ones fitted for the NaA and NaLSX zeolites [43], for which most of the estimates were around 3 MHz. Having no experimental data on the bridged ^{17}O atom connected to a proton, we then concluded that the respective C_{QQ} for the Si–O(H)–Al oxygens should be larger than those for the Si–O–Al moiety and hence would lead to a broadening of the respective lines in the NMR spectra. The EFG anisotropy η did not reveal any difference between the Si–O–Al and Si–O–Si types of oxygen. Most of the obtained η values for the Si–O–Si and Si–O–Al moieties are below 0.4. Only the O atoms of the Si–O(H)–Al type are characterized by higher η values around 0.9.

The variation of $C_{QQ}(^{17}O)$ with the elongation of the O–H bond for the Si–O(H)–Al moiety, as could be observed, for example, when the H is coordinated to an adsorbed particle, has to our knowledge never been discussed in the literature. However, it has been shown that the $C_{QQ}(^{27}Al)$ values of a loaded sample decrease by 2–3 orders of magnitude as compared to the value for the nonloaded case [26] owing to the simultaneous increase of the O–H bond length as well as to the decrease of the O–Al bond upon H coordination. The H atom is very close to the oxygen and its influence is thus important. Hence, the theoretical evaluation of $C_{QQ}(^{17}O)$ with respect to the O–H bond length becomes very useful. We found that both the $C_{QQ}(^{17}O)$ and $\eta(^{17}O)$ variations are less than a few percent under elongation from 0.9833 to 1.0333 Å, which is usually smaller than the experimental error. This slight dependence demonstrates the importance of

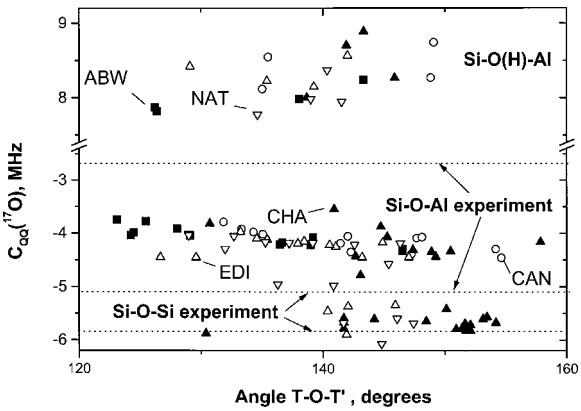

FIGURE 4. $C_{QQ}(^{17}O)$ (in MHz) with respect to T–O–T′ angle (in degrees) in the Si–O–Si, Si–O–Al, and Si–O(H)–Al moieties, calculated with ps-21G** for the five H-form aluminosilicates. Intervals of experimental data [39–43] for the Si–O–Si and Si–O–Al moieties are limited by dashed lines.

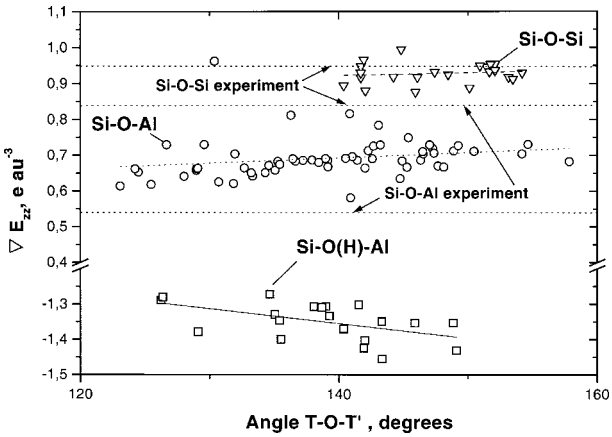

FIGURE 5. EFG $\nabla E_{zz}(^{17}O)$ (in $e \times$ a.u.$^{-3}$) with respect to T–O–T′ angle (in degrees) in the Si–O–Si, Si–O–Al, and Si–O(H)–Al moieties calculated with ps-21G** for the five H-form aluminosilicates. Intervals of experimental data for the Si–O–Si and Si–O–Al moieties, recalculated from the known $C_{QQ}(^{17}O)$ values [39–43], are limited by dashed lines.

the contributions of the Si and Al neighbors, which possess higher atomic charges than the hydrogen, to the total EFG value at the O position. The small $C_{QQ}(^{17}O)$ change with the O–H stretching cannot be measured; however, it should be verified allowing an additional charge transfer of the electronic density to the H-bonded molecule, which was not considered in our calculations.

Conclusions

Quadrupole coupling constants C_{QQ} of the crystallographically different ^{2}H, different ^{27}Al, and different ^{17}O atoms were obtained for a series of "small" size H-form aluminosilicate models (ABW, CAN, CHA, EDI, NAT) optimized with periodic Hartree–Fock calculations at the STO-3G level using the CRYSTAL code. Single-point calculations were then carried out at the ps-21G*(Al, Si)/6-21G*(O, H) and 6-21G*(Al, Si)/6-21G*(O, H) levels.

Resulting $C_{QQ}(^{27}Al)$ values depend on both deformational (O–Al–O) and valence (O–Al) distortions of the AlO_4 tetrahedra in the H-forms. Long-range contributions to the EFG ∇E_{zz} (^{27}Al) calculated with a periodic Hartree–Fock scheme provide more precise estimations to the $C_{QQ}(^{27}Al)$ than a cluster approach at the same basis set level.

The $C_{QQ}(^{17}O)$ values for the Si–O–Si and Si–O–Al moieties coincide with the respective data measured for the X and Y cationic forms and silicates. It thus confirms the correct representation of the derivatives of the electrostatic potential on the ^{17}O nuclei using the ps-21G*(Al, Si)/6-21G*(O, H) basis set. Correlations of the $C_{QQ}(^{17}O)$ values with the respective T–O–T′ angle were too weak and hence did not allow any quantitative reasoning in accordance with the recent results presented in [40].

For all variety of Si–O(H)–Al moieties (including the case corresponding to a cluster geometry), $C_{QQ}(^{2}H)$ coincided with the experimental data for the HY and HZSM-5 forms if the anharmonicity effects of the O–^{2}H bond are taken into account. We also showed that a precise β angle value of the H deflection from the Si–O–Al plane should be considered to connect the absolute value of the electrostatic field/OH frequency with the local geometry of the bridged group.

The agreement between the C_{QQ} values of all considered atoms for the small size H-form aluminosilicates (ABW, CAN, CHA, EDI, NAT) with the values measured for "large" size forms (ZSM-5, Y) suggests a similar electrostatic "media" in which the framework atoms are embedded. This confirms the possibility to describe their properties (like atomic moments) within a similar approach, i.e., a common dependence on geometry and low-order multipole moments for the atoms of small and large size zeolites as proposed in [7].

Cationic forms were shown to be more appropriate initial structures than their siliceous analogs for optimization of the geometry because they require a smaller perturbation of the cell parameters. The cationic forms are thus useful when one does not require a comparison of the H-form characteristics with respect to the basic siliceous structures.

ACKNOWLEDGMENTS

The authors wish to thank the FUNDP for the use of the Namur Scientific Computing Facility (SCF) Centre, a common project between the FNRS, IBM-Belgium, and FUNDP as well as MSI for the use of their data in the framework of the "Catalysis and Sorption" consortium. We are grateful for the partial support of the Interuniversity Research Program on "Reduced Dimensionality Systems" (PAI/IUAP 4/10) initiated by the Belgian Government. The authors are grateful to Prof. J. Sauer and Dr. F. Jousse for useful discussions.

References

1. B. Nagy, J.; Bodart, P.; Hannus, I.; Kiricsi, I. Synthesis, Characterization and Use of Zeolitic Microporous Materials; DecaGen: Szeged-Szoreg, Hungary, 1998.
2. Koller, H.; Engelhardt, G.; van Santen, R. A. Topics in Catalysis 1999, 9, 163.
3. Brown, A. S.; Spackman, M. A. Mol Phys 1994, 83, 551.
4. Stewart, R. F. Chem Phys Lett 1979, 65, 335.
5. Cohen de Lara, E.; Delaval, Y. J Chem Soc Faraday Trans II 1978, 74, 790.
6. Marra, G. L.; Fitch, A. N.; Zecchina, A.; Ricchiardi, G.; Salvalaggio, M.; Bordiga, S.; Lamberti, C. J Phys Chem B 1997, 101, 10653.
7. Larin, A. V.; Vercauteren, D. P. Int J Quantum Chem, to appear.
8. Pisani, C.; Dovesi, R.; Roetti, C. Hartree–Fock Ab Initio Treatment of Crystalline Systems; Springer: New York, 1988.
9. Saunders, V. R.; Freyria-Fava, C.; Dovesi, R.; Salasco, L.; Roetti, C. Mol Phys 1992, 77, 629.
10. Krogh Andersen, E.; Ploug-Sorensen, G. Zeit Kristallogr 1986, 176, 67.
11. Bresciani Pahor, N.; Calligaris, M.; Nardin, G.; Randaccio, L. Acta Cryst 1982, B38, 893.
12. Teunissen, E. Ph.D. Thesis, Univ. of Eindhoven, The Netherlands, 1994.

13. Galli, E. Acta Cryst 1976, B32, 394.
14. Pechar, F.; Schafer, W.; Will, G. Zeit Kristallogr 1983, 164, 19.
15. Larin, A. V.; Vercauteren, D. P. J Mol Catal A 2001, 168, 123.
16. Dovesi, R.; Saunders, V. R.; Roetti, C.; Causà, M.; Harrison, N. M.; Orlando, R.; Aprà, E. CRYSTAL95 1.0, User's Manual, 1996.
17. Press, W. H.; Flannery, B. P.; Teukolsky, S. A.; Wetterling, W. T. Numerical Recipes; Cambridge University Press: New York, 1988.
18. Sundholm, D.; Olsen, J. Phys Rev Lett 1992, 68, 927.
19. Sundholm, D.; Olsen, J. J Phys Chem 1992, 96, 627.
20. Reid, R. V.; Vaida, M. L. Phys Lett 1973, A7, 1841.
21. Bishop, D. M.; Cheung, L. M. Phys Lett 1979, A20, 381.
22. Fenzke, D.; Hunger, M.; Pfeifer, H. J Magn Res 1991, 95, 477.
23. Ugliengo, P.; Civalleri, B.; Dovesi, R.; Zicovich-Wilson, C. M. Phys Chem Chem Phys 1999, 1, 545.
24. Gale, J. D. GULP (The General Utility Lattice Program), Royal Institution Imperial Colledge, UK, 1992/1994.
25. Ernst, H.; Frede, D.; Wolf, I. Chem Phys Lett 1993, 212, 588.
26. Hunger, M.; Horvath, T. J Am Chem Soc 1996, 118, 12302.
27. Czjzek, M.; Jobic, H.; Fitch, A. N.; Vogt, T. J Phys Chem 1992, 96, 1535.
28. Buckingham, A. D. Trans Faraday Soc 1960, 753.
29. Hulburt, H. M.; Hirschfelder, J. O. J Chem Phys 1941, 9, 61.
30. International Tables for X-ray Crystallography; Kynoch Press: Birmingham, UK, 1962; Vol. 3, p. 272.
31. Jeanvoine, Y.; Ángyán, J. G.; Kresse, G.; Hafner, J. J Phys Chem 1998, B102, 5573.
32. Sastre, G.; Lewis, D. W. J Chem Soc Faraday Trans 1998, 94, 3049.
33. Sastre, G.; Lewis, D. W.; Corma, A. Phys Chem Chem Phys 2000, 2, 177.
34. Sastre, G.; Fornes, V.; Corma, A. Chem Comm 1999, 2163.
35. Civalleri, B.; Ugliengo, P.; Zicovich-Wilson, C. M.; Harrison, N. M.; Dovesi, R. 8th International Conference on the Theoretical Aspects of Heterogeneous Catalysis, La Colle sur Loup, France, May 30–June 6, 2000, p. 9.
36. Ghose, S.; Tsang, J. Am Mineral 1973, 58, 748.
37. Kellö, V.; Sadlej, A. J.; Pyykkö, P.; Sundholm, D.; Tokman, M. Chem Phys Lett 1999, 414, 304.
38. Koller, H.; Meijer, E. L.; van Santen, R. A. Solid State Nucl Magn Res 1997, 9, 165.
39. Bull, L. M.; Cheetham, A. K.; Anupold, T.; Reinhold, A.; Samoson, A.; Sauer, J.; Bussemer, B.; Lee, Y.; Gann, S.; Shore, J.; Pines, A.; Dupree, R. J Am Chem Soc 1998, 120, 3510.
40. Bull, L. M.; Bussemer, B.; Anupold, T.; Reinhold, A.; Samoson, A.; Sauer, J.; Cheetham, A. K.; Dupree, R. J Am Chem Soc 2000, 122, 4948.
41. Schramm, S.; Kirkpatrick, R. J.; Oldfield, E. J Am Chem Soc 1983, 105, 2483.
42. Mueller, K. T.; Wu, Y.; Chmelka, B. F.; Stebbins, J.; Pines, A. J Am Chem Soc 1991, 113, 32.
43. Pingel, U.-T.; Amoureux, J.-P.; Anupold, T.; Bauer, F.; Ernst, H.; Fernandez, C.; Freude, D.; Samoson, A. Chem Phys Lett 1998, 294, 345.